Cumhuriyet Sci. J., 43(4) (2022) 752-759
DOI: https://doi.org/10.17776/csj.1180411

Cumhuriyet Science Journal

| csj.cumhuriyet.edu.tr | Founded: 2002 ISSN: 2587-2680 e-ISSN: 2587-246X Publisher: Sivas Cumhuriyet University

Effects of Deuteron and Alpha Optical Model Potentials on the Production Cross–Section Calculations of Some Radiobromine Isotopes

Mert Şekerci[1,a,*], Abdullah Kaplan[1,b]

[1] *Department of Physics, Süleyman Demirel University, Isparta, Türkiye*
**Corresponding author*

Research Article

History
Received: 26/09/2022
Accepted: 28/11/2022

ABSTRACT

The extensive use of radioisotopes in diverse fields, particularly in medical studies for diagnosis and treatment, is one of the outcomes of evolving technology and improved scientific research. Among the various radioisotopes used for medical purposes, an example that can be highlighted considering their properties and utilization possibilities is radiobromine isotopes. It is obvious that both experimental and theoretical studies make significant contributions to the literature on medically relevant radioisotopes. The cross–section, which is the data connected with the occurrence of a reaction, is one of the theoretical metrics that may provide information to researchers. The framework of this study was constructed by taking into account the importance of radiobromine isotopes in medical applications as well as the effects of some parameters that might have an impact on their production cross–section calculations. In this context, the impact of five deuteron and eight alpha optical model potentials, which are available in the 1.95 version of the TALYS code, on the production cross–section calculations of $^{75\text{-}77}$Br radioisotopes through some (d,x) and (α,x) reactions have been studied. The obtained calculation results were compared visually and numerically with the experimental data available in the literature for each reaction, and the outputs were interpreted.

Keywords: Alpha optical model potential, Cross–section, Deuteron optical model potential, Radiobromine, TALYS

[a] *mertsekerci@sdu.edu.tr* *https://orcid.org/0000-0003-0870-0506* [b] *abdullahkaplan@sdu.edu.tr* *https://orcid.org/0000-0003-2990-0187*

Introduction

The studies that contribute the most to the literature in basic sciences, engineering, medicine and many other fields may seem like experimental studies. However; with a deeper analysis, it can be easily understood that the studies that contribute to the literature are not only experimental studies. It should be considered normal that studies with results that can be integrated into industrial applications in general and people's daily lives in particular attract more attention and that such studies can take place more easily in the literature. The reason for this could be given as the fact that the results of such studies can be used more quickly and are useful in achieving outcomes that can benefit huge groups of people. Nevertheless, the idea that this situation can only be achieved through experimental studies is not entirely correct. Experimental studies are mostly dependent on many parameters such as advanced technological infrastructure, availability of trained people and workforce, large and comfortable financial budgets and effective time management. Furthermore, all of these elements should function in unison. For this reason, it is possible to encounter many problems during the planning and implementation of an experimental study and analyzing the results and converting them into outputs. In such cases, it is extremely important for researchers to obtain information about the studies they plan to carry out. This is valid in all branches of science, albeit to varying degrees. For this reason, theoretical studies are as important as experimental studies and contribute to the literature. In this context, as in many research areas, theoretical studies carried out according to the content of the planned research are accepted in the literature in studies related to radioisotopes, which are the subject of this study.

Radioisotopes are actively used in a very wide area of modern human life. For example, some of the industrial applications include Carbon-14 used for age determination of carbon-containing structures, Americium-241 used in smoke detectors, Cobalt-60 used in gamma sterilization and industrial radiography, Iridium-192 used in the determination of defects in metal components by gamma radiography, Selenium-75 used in gamma radiography and non-destructive testing and many more [1]. Apart from these radioisotopes, which can be shown as examples in the industrial field, many radioisotopes are used for diagnosis and treatment in many medical applications, considering their characteristics and benefits [2]. In this context, it was necessary to use not only reactors but also accelerators in order to provide supply-demand balance for radioisotopes, which are increasingly used in the medical field. As a result, the production of radioisotopes in accelerators, which are used for diagnostic purposes such as imaging and clinical purposes such as treatment, could be achieved by bombardment of charged particles. From this point of view, it is extremely possible to come across

studies in the literature that experimentally examine the production routes of radioisotopes used in the medical field. On the other hand, there are also theoretical studies investigating the effects of many models and parameters in the calculation of various values such as cross–section, particle emission spectrum, activity and yield in many reactions, including the production routes of various radioisotopes [3-9].

It is a well–known fact that many computable values are extremely important in the theoretical analysis of a reaction. Some values can be measured both experimentally and theoretically. The cross–section, which is defined as a value of the scale of the realization of a reaction, is also a quantity that can be obtained both experimentally and theoretically [10]. Cross–section data is extremely valuable to study the behavior of the reaction in regions outside of the feasible experimental energy range, or the target-incoming particle relationship, to study many special cases. In this context, the improvement of the models on which the calculations are based by comparing the cross–section values obtained with the theoretical calculations with the experimental data, or the investigation of the effects of various parameters on these calculations are seen as very valuable studies. There are many models and parameters that are known to have an impact on cross–section calculations. Level density models, gamma strength functions, deuteron and alpha optical model potentials can be given as examples. Studies examining the use of these models and parameters independently or in combination to produce results that are more compatible with experimental data also contribute to the literature [11-20]. The motivation of this study was created in this conjuncture. In this direction, it is aimed to examine the effects of the deuteron and alpha optical model potentials in the production cross–section calculations of 75-77Br radioisotopes, which are known to be used in the medical field, with some (d,x) and (α,x) reactions. The results of the calculations for the reactions examined in this study were compared with the experimental data available in the literature and the outcomes were interpreted. While trying to make a visual comparison of the naked eye with the graphics in which the current experimental data and the calculation results are presented together, statistical parameters are used to make quantitative comparisons at the same time.

Materials and Methods

This section will give information regarding the chosen material and the method employed within the context of the primary motivation for this study. This chapter can be divided into two sections in this sense. The first section will attempt to explain why certain radiobromine isotopes are selected. Following that, the models utilized in the calculations, the calculating tools, and how the results are assessed will be discussed.

Some of the many radioisotopes used in medical studies belong to bromine. Bromine, with atomic number 35 and symbolized by Br, is the third lightest halogen. Bromine, which was introduced to the literature in 1825 and 1826 by two independent researchers, occurs in nature as bromide salts or organobromine compounds [21, 22]. Bromine has two stable isotopes, ^{79}Br and ^{81}Br, with abundances of 51 % and 49 %, respectively. Apart from these, it has 32 known radioisotopes, the most stable being ^{77}Br [23]. Among all known radioisotopes, the most preferred ones in medical applications are $^{75\text{-}77}$Br radioisotopes. The decay modes of ^{75}Br are known as approximately 73 % positron emission (β^+) and approximately 27 % electron capture (EC). ^{75}Br, with a half-life of approximately 96.7 minutes, can form particles with a maximum energy of 2.008 MeV and an average of 0.719 MeV with positron emission. The half-life of ^{76}Br is about 16.2 hours, and its decay modes are positron capture and electron capture at approximately 55 % and 45 %, respectively. In case of decay by positron capture from these possibilities, it can form positrons with an average energy of 1.180 MeV, and the energy of these particles can go up to a maximum of 3.941 MeV. Another radioisotope examined in this study is ^{77}Br, which has a much longer half-life, 57.036 hours, than the other two. On the other hand, ^{77}Br is the radioisotope with the lowest decay rate by positron emission, 0.74 %, and the highest decay rate by electron capture, 99.26 %, among the $^{75\text{-}77}$Br radioisotopes. The average and highest positron emission values of ^{77}Br are 0.152 MeV and 0.343 MeV, respectively [24]. The use of $^{75\text{-}77}$Br radioisotopes in medical applications has been accepted in the literature as a result of their characteristic properties and many related parameters. ^{75,76}Br radioisotopes are generally used for Positron Emission Tomography (PET) purposes, as they have a higher rate of positron emission decay and the positrons produced in decay are at moderate energies, while ^{77}Br is mostly used for Auger therapy as an advantage of its high rate of electron capture decay [25].

$^{75\text{-}77}$Br radioisotopes were planned to be selected within the scope of this study, considering their usability in medical applications and the benefits they provide. The literature has been searched for the experimental studies that cover the production routes of these radioisotopes. As a result, the desire to investigate the implications of theoretical models by performing production cross–section calculations in various reactions where deuterons or alphas were selected as the incident particle was developed. In this context, it is aimed to obtain the production cross-section calculations with deuteron and alpha optical model potentials in accordance with the examined reaction and to interpret the results by comparing them with the experimental data available in the literature. The cross–section value, as explained in the previous section, is a value that can be obtained experimentally and can be calculated with theoretical models under the influence of various parameters. The TALYS [26] code v1.95 was used to investigate the effects of deuteron and alpha optical model potentials on the generation cross–section calculations in accordance with the (d,x) and (α,x) reactions examined in this study. Since

cross–section calculations require multistage and complex operations, codes such as TALYS have always been needed. In this context, although many codes such as CEM95, ALICE-91, ALICE/ASH, PCROSS and EMPIRE have been developed, it can be understood even with a quick and superficial examination that TALYS is the most preferred code in the literature. The reason for this can be shown as the code's accessibility, ease of use, comprehensive user guide and options that it provides to users, allowing advanced calculation and examination processes compared to other alternatives. In addition, numerous studies examining the effects of various models and parameters on the theoretical acquisition of different values, especially the cross–section, with the mentioned code can be easily seen in the literature, as shown in the citations given earlier in the text. Considering all these, it was decided to use the TALYS code version 1.95 in this study.

The mentioned code accepts the pre-equilibrium reaction mechanism as the default for the incoming particle energies above the last discrete level energy of the target nucleus, among the equilibrium and pre–equilibrium reaction mechanism options in cross–section calculations. In addition, the two–component exciton model is also active in calculations by default and utilized for the calculations that performed within the scope of this study. All details are defined with keywords in the input file of the code. It is possible to activate/deactivate the equilibrium or pre-equilibrium reaction mechanism by the user, or it is possible to select the desired one among four different pre-equilibrium reaction mechanisms. The default model uses the energy dependent matrix element and the exciton model using numerical transition ratios. As a result of the inclusion of different parameters into the input file of the code by the user, it is possible to examine their effects on the calculations. The parameters that constitute the motivation of this study are related to the optical model. The concept of level density model is also refers to another very important factor for similar investigations. In this study, the Constant temperature+Fermi gas model (CTFGM), which was also assigned as the default one within the utilized code, was accepted in all calculations. Turning back to the optical model, the basic assumption underlying the optical model is that the sophisticated interaction between the incoming particle and the nucleus can be represented by a complex mean field potential. This complex mean field potential divides the reaction flow into two parts, which are grouped into the part covering the elastic scattering pattern and all the remaining inelastic channels. The reaction cross–section values calculated with optical models are also very important for semi-classical pre-equilibrium models, and therefore, the examination of optical models is a contribution to the literature [26]. There are different number of deuteron and alpha optical model potential options that can be utilized in the calculations performed via the TALYS v1.95 code. All deuteron and alpha optical model potential options are shown in Tables 1 and 2, respectively, with their names and abbreviations used in this study.

Table 1. The names and abbreviations of the deuteron optical model potentials

The name of the deuteron optical model potential	Abbreviation used in this study
Normal Deuteron Potential	DOMP1
Deuteron potential of [27]	DOMP2
Deuteron potential of [28]	DOMP3
Deuteron potential of [29]	DOMP4
Deuteron potential of [30]	DOMP5

Table 2. The names and abbreviations of the alpha optical model potentials

The name of the alpha optical model potential	Abbreviation used in this study
Normal Alpha Potential	AOMP1
Alpha potential of [31]	AOMP2
Table 1 of [32]	AOMP3
Table 2 of [32]	AOMP4
Dispersive model of [32]	AOMP5
Avrigeanu et al. [33]	AOMP6
Nolte et al. [34]	AOMP7
Avrigeanu et al. [35]	AOMP8

The impacts of the deuteron optical model potentials provided in Table 1 in reactions ^{nat}Se(d,x)^{75}Br, ^{nat}Se(d,x)^{76}Br and ^{nat}Se(d,x)^{77}Br, as well as the effects of the alpha optical model potentials shown in Table 2 in reactions ^{74}Se(α,x)^{75}Br, ^{74}Se(α,x)^{76}Br, ^{76}Se(α,x)^{77}Br and ^{77}Se(α,x)^{77}Br, were explored in this work. Calculations were made by using only one deuteron or alpha optical model potential in the calculation at a time, depending on the type of particle involved for each reaction. After the calculations were completed with the appropriate optical models (deuteron or alpha) for each reaction, the results obtained were graphed together with the experimental data so that they could be analyzed visually. In addition, some statistical parameters have been calculated so that quantitative analyzes can be made with numerical values, going beyond just making visual interpretations with the naked eye. The equations that were employed in these computations in where *F*, *D*, *R* and *K* represents the mean standardized deviation, the mean relative deviation, the mean ratio and the mean square logarithmic deviation, respectively, are listed below [36].

$$F = \left[\frac{1}{N}\sum_{i=1}^{N}\left[\frac{\sigma_i^{cal} - \sigma_i^{exp}}{\Delta\sigma_i^{exp}}\right]^2\right]^{1/2}$$

$$D = \left[\frac{1}{N}\sum_{i=1}^{N}\left|\sigma_i^{cal} - \sigma_i^{exp}\right|/\sigma_i^{exp}\right]$$

$$R = \left[\frac{1}{N}\sum_{i=1}^{N}\frac{\sigma_i^{cal}}{\sigma_i^{exp}}\right]$$

$$K = 10^{\left[\frac{1}{N}\sum_{i=1}^{N}\left[\log(\sigma_i^{exp}) - (\sigma_i^{cal})\right]^2\right]^{1/2}}$$

In the equations given for *F*, *D*, *R* and *K*, σ_i^{exp} and σ_i^{cal} express the experimental and calculated cross–section values,

respectively, while $\Delta\sigma_i^{exp}$ expresses the instability value of each experimental cross–section value, in other words, the amount of error.

Results and Discussion

Within the scope of this study, which was clearly explained in the previous sections, cross–section calculations were completed by triggering the possible deuteron and alpha optical model potentials in the calculations performed by utilizing the TALYS code version 1.95. Obtained calculation results and experimental data are illustrated in Figures 1-7. In addition, the values of the statistical parameters calculated in order to perform a numerical analysis between the experimental data and the calculation results are shown in Tables 3 and 4.

For the reactions of $^{nat}Se(d,x)^{75}Br$, $^{nat}Se(d,x)^{76}Br$ and $^{nat}Se(d,x)^{77}Br$, the experimental data obtained from the study of Tárkányi et al. [37] available in the literature and from EXFOR [38, 39] were used. As can be seen from the results graphed in Figures 1-3, the theoretical calculations for all three reactions were generally able to generate geometric structures similar to those of the experimental data.

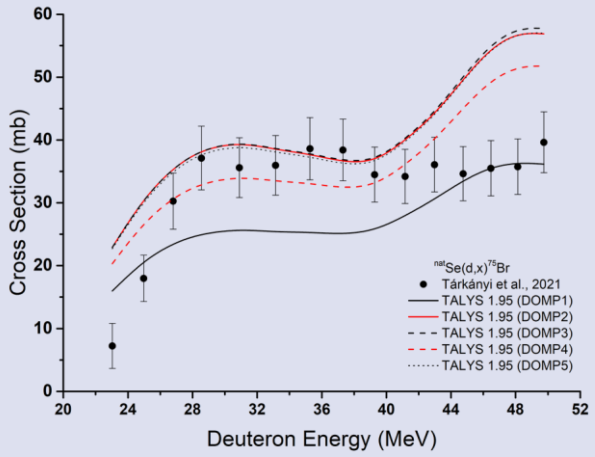

Figure 1. Experimental data along with the calculations results for $^{nat}Se(d,x)^{75}Br$ reaction

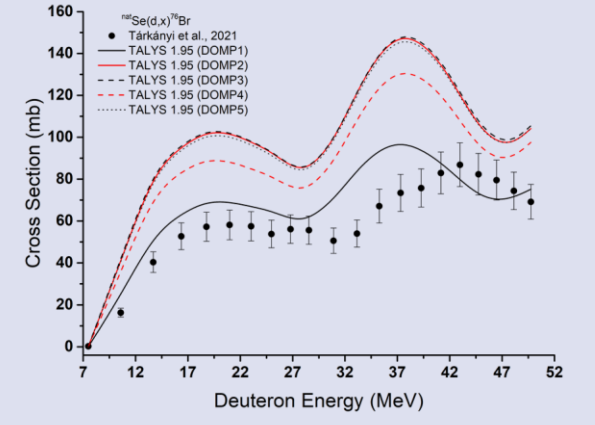

Figure 2. Experimental data along with the calculations results for $^{nat}Se(d,x)^{76}Br$ reaction

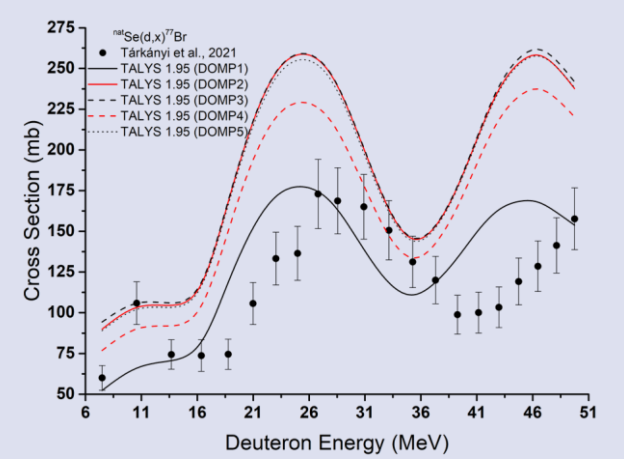

Figure 3. Experimental data along with the calculations results for $^{nat}Se(d,x)^{77}Br$ reaction

There have been observations of results that are not expected to be absolutely and exactly the same as experimental data. Furthermore, the calculation results of the models represented by DOMP2, DOMP3, and DOMP5 in all three reactions were produced in such a way that they were exceptionally close and consistent with one another. The values of the statistical parameters shown in Table 3 also help us understand the circumstance.

Using the DOMP2, DOMP3 and DOMP5 models, higher cross–section values were obtained in the $^{nat}Se(d,x)^{76}Br$ and $^{nat}Se(d,x)^{77}Br$ reactions than almost all of the experimental data, and in the $^{nat}Se(d,x)^{75}Br$ reaction than most of the experimental data. When the values of the *F*, *D*, *R* and *K* parameters are considered together, the deuteron optical model, which provides the most compatible results with the experimental data for the $^{nat}Se(d,x)^{75}Br$ and $^{nat}Se(d,x)^{77}Br$ reactions, is referred as DOMP1. For the $^{nat}Se(d,x)^{76}Br$ reaction, the *F*, *D* and *R* values highlight DOMP1, while the *K* value suggests that DOMP4 is the model that produces the most consistent results with the experimental data. Components used in the calculation of statistical parameters and sequence of operations can be cited as the reason for this difference. In addition, the logarithmic operation in the *K* value can be shown as an important factor for this difference.

Levkovski [40]'s experimental data were used in the $^{74}Se(\alpha,x)^{75}Br$, $^{74}Se(\alpha,x)^{76}Br$, $^{76}Se(\alpha,x)^{77}Br$ and $^{77}Se(\alpha,x)^{77}Br$ reactions in which the effects of alpha optical model parameters were investigated. Obtained calculation results and experimental data are shown together in Figures 4-7.

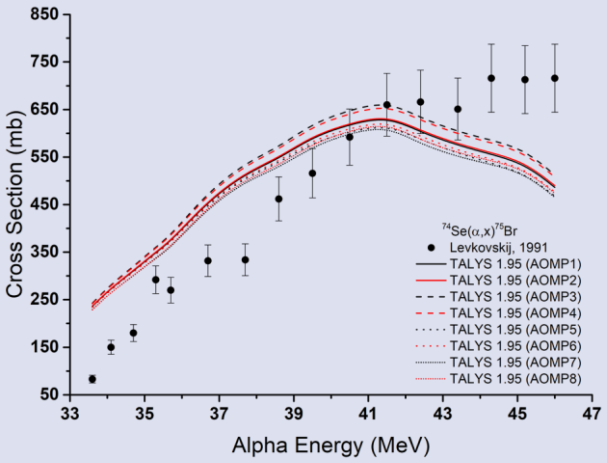

Figure 4. Experimental data along with the calculations results for $^{74}Se(\alpha,x)^{75}Br$ reaction

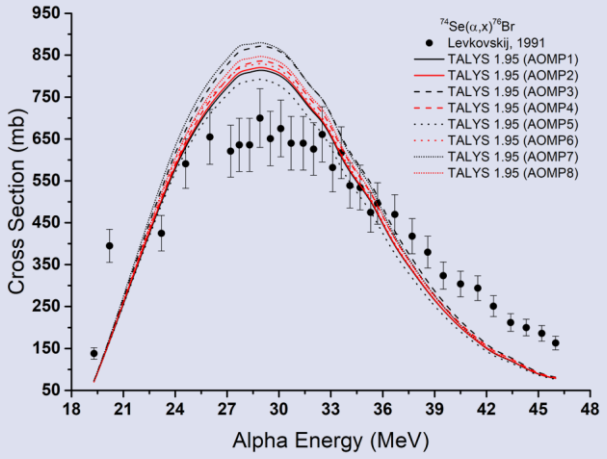

Figure 5. Experimental data along with the calculations results for $^{74}Se(\alpha,x)^{76}Br$ reaction

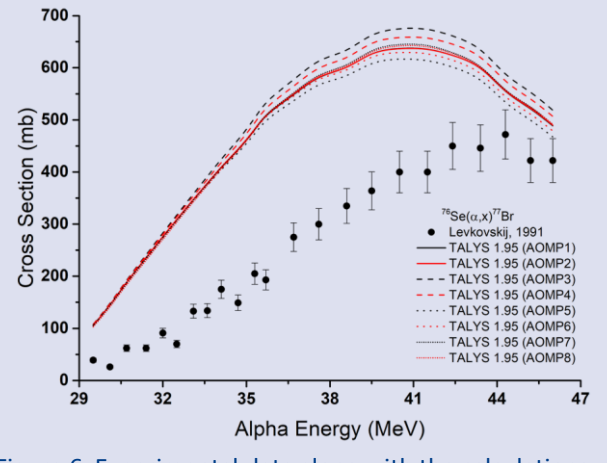

Figure 6. Experimental data along with the calculations results for $^{76}Se(\alpha,x)^{77}Br$ reaction

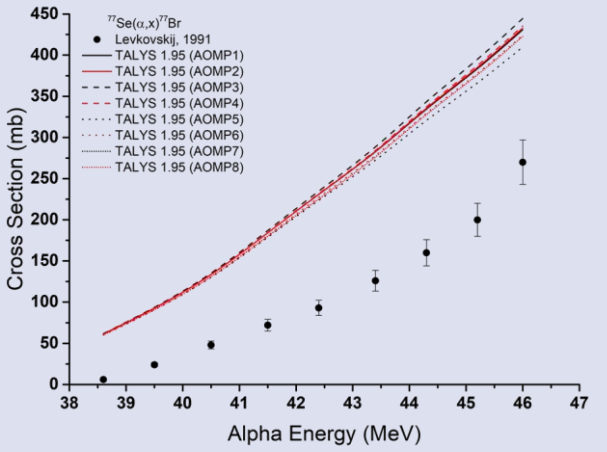

Figure 7. Experimental data along with the calculations results for $^{77}Se(\alpha,x)^{77}Br$ reaction

The values of the statistical parameters for the alpha optical model potentials were determined in the same way as they were for the deuteron optical model potentials, and the results are shown in Table 4.

Table 3. The values of the statistical parameters calculated for deuteron optical model potentials

Reaction	Statistical parameters	DOMP1	DOMP2	DOMP3	DOMP4	DOMP5
$^{nat}Se(d,x)^{75}Br$	F	1.767	2.662	2.729	1.992	2.632
	D	0.260	0.386	0.392	0.300	0.378
	R	0.924	1.376	1.383	1.224	1.366
	K	1.389	1.491	1.496	1.401	1.485
$^{nat}Se(d,x)^{76}Br$	F	2.342	6.614	6.728	5.044	6.463
	D	0.256	0.758	0.772	0.573	0.742
	R	1.127	1.664	1.678	1.479	1.648
	K	2.965	2.924	2.902	2.877	2.918
$^{nat}Se(d,x)^{77}Br$	F	2.561	6.268	6.376	5.064	6.168
	D	0.248	0.650	0.664	0.506	0.636
	R	1.136	1.650	1.664	1.490	1.636
	K	1.312	1.705	1.718	1.567	1.693

Table 4. The values of the statistical parameters calculated for alpha optical model potentials

Reaction	Statistical parameters	AOMP1	AOMP2	AOMP3	AOMP4	AOMP5	AOMP6	AOMP7	AOMP8
$^{74}Se(\alpha,x)^{75}Br$	F	5.872	5.908	6.203	6.140	5.829	5.797	5.573	5.568
	D	0.394	0.396	0.414	0.409	0.394	0.391	0.376	0.375
	R	1.263	1.269	1.315	1.305	1.244	1.250	1.221	1.229
	K	1.490	1.492	1.509	1.505	1.493	1.488	1.476	1.473
$^{74}Se(\alpha,x)^{76}Br$	F	2.952	2.961	3.079	2.953	2.991	3.013	3.227	3.062
	D	0.244	0.247	0.273	0.251	0.240	0.254	0.287	0.264
	R	0.917	0.923	0.984	0.946	0.885	0.931	0.977	0.951
	K	1.466	1.463	1.449	1.450	1.487	1.469	1.480	1.470
$^{76}Se(\alpha,x)^{77}Br$	F	17.647	17.668	18.408	18.127	17.460	17.398	17.510	17.224
	D	1.402	1.404	1.493	1.457	1.367	1.378	1.398	1.379
	R	2.402	2.404	2.493	2.457	2.367	2.378	2.398	2.379
	K	2.437	2.439	2.517	2.485	2.410	2.417	2.433	2.414
$^{77}Se(\alpha,x)^{77}Br$	F	34.083	33.991	34.463	34.074	33.145	33.350	33.315	33.198
	D	2.296	2.294	2.343	2.3041	2.202	2.239	2.230	2.236
	R	3.296	3.294	3.343	3.304	3.202	3.239	3.230	3.236
	K	3.136	3.136	3.179	3.144	3.054	3.089	3.080	3.087

It can be seen from Figure 4 that the results obtained using alpha optical model potentials in the $^{74}Se(\alpha,x)^{75}Br$ reaction and the experimental data are relatively similar. The alpha optical model potential, which produces the computational results most compatible with the experimental data for this reaction, is pointed as AOMP8 by the *F*, *D*, and *K* values, while the *R* value suggests AOMP7. We are now in the part where we will examine the results related to the $^{74}Se(a,x)^{76}Br$ reaction. In this reaction, where the calculation results and the experimental data are shown in Figure 5, it can be seen that the calculation results differ from each other at the top of the hump structure to such an extent that they can be noticed even with the naked eye, but they produce results that are very close to each other in other regions. Higher values of cross–section were obtained than experimental data in the energy range of roughly 24-36 MeV, and this condition changed when the calculation results dropped below the experimental values after approximately 36 MeV. In the $^{74}Se(\alpha,x)^{76}Br$ reaction, *D* and *R* values highlight AOMP5, *F* value indicates AOMP1, and *K* value indicates AOMP3. This disparity may have happened because the cross–section value at each energy point has a distinct level of experimental error, while the statistical parameters look at the full energy range.

Table 5. The arithmetic averages of the statistical parameters of the deuteron optical model potentials

Statistical parameters	DOMP1	DOMP2	DOMP3	DOMP4	DOMP5
F	2.223	5.182	5.277	4.033	5.088
D	0.255	0.598	0.609	0.460	0.585
R	1.062	1.564	1.575	1.397	1.550
K	1.889	2.040	2.039	1.948	2.032

Table 6. The arithmetic averages of the statistical parameters of the alpha optical model potentials

Statistical parameters	AOMP1	AOMP2	AOMP3	AOMP4	AOMP5	AOMP6	AOMP7	AOMP8
F	15.138	15.132	15.538	15.324	14.856	14.890	14.906	14.763
D	1.084	1.085	1.131	1.105	1.051	1.066	1.073	1.063
R	1.969	1.972	2.034	2.003	1.925	1.950	1.957	1.949
K	2.132	2.132	2.163	2.146	2.111	2.116	2.117	2.111

Another radiobromine isotope examined in the study is ^{77}Br, and two reactions were investigated for the production of this radioisotope with alpha-input particles, $^{76}Se(\alpha,x)^{77}Br$ and $^{77}Se(\alpha,x)^{77}Br$. In both of these reactions, the experimental data of Levkovski [40] and the calculation results were visualized together and the graphs obtained are shown in Figures 6 and 7. As can be clearly seen from these figures, triggering of alpha optical model potentials in both reactions caused higher cross–section values to be calculated than the experimental data at all energy values. As the energy value increased along the x-axis, the distance between the cross–section results obtained via the alpha optical model potentials are widened. In the $^{76}Se(\alpha,x)^{77}Br$ reaction, the *F* value suggests that if AOMP8 is used, more consistent results can be obtained with the experimental data, while the *D*, *R* and *K* values show that such situation can be achieved by using AOMP5. On the other hand, all statistical parameters for the $^{77}Se(\alpha,x)^{77}Br$ reaction point to the same alpha optical model potential, AOMP5.

Conclusion

It is a well–known fact that the cross–section value is valuable in terms of the contributions it provides to researchers in cases where experimental studies cannot be performed. From this point of view, the selection of models and appropriate parameters that can produce results that are more compatible with the experimental data is extremely critical. The results of this study, which was designed by considering the importance of radiobromine isotopes, that have a wide range of use in

motivation and health applications, can be summarized as follows.

- It has been demonstrated that activating the deuteron and alpha optical model potentials in cross–section calculations alters the calculation results.

- The cross–section values produced in this work employing deuteron and alpha optical model potentials contributed to the literature.

- Specific to the reactions studied, multiple statistical parameters were used to determine the option that produced more consistent results with the experimental data among all deuteron and alpha optical model potentials included in the calculations. As a result, it was seen that all statistical parameters in $^{nat}Se(d,x)^{75}Br$, $^{nat}Se(d,x)^{77}Br$ and $^{77}Se(\alpha,x)^{77}Br$ reactions point to the same optical model potential. The value of one statistical parameter in each of these three reactions, *K* in reaction $^{nat}Se(d,x)^{76}Br$, *R* in reaction $^{74}Se(\alpha,x)^{75}Br$, and *F* in reaction $^{76}Se(\alpha,x)^{77}Br$, highlighted a different optical model potential from the others. While *D* and *R* values imply the same optical model potential in reaction $^{74}Se(\alpha,x)^{76}Br$, triggering various optical model potentials in the computations yields findings that are more congruent with the experimental data with respect to *F* and *K* values.

- The arithmetic averages of the statistical parameters of the deuteron optical model potentials are provided in Table 5. According to these values, in the reactions where the effects of the deuteron optical model potentials were examined, all statistical parameters (*F*, *D*, *R* and *K*) showed DOMP1 as the option that provided more consistent results with the experimental data compared to the other options.

- A situation similar to that in Table 5 is presented in Table 6 for alpha optical model potentials. When the results here are examined, the model that produces more compatible results compared to the experimental data and other alpha optical model potentials is AOMP8 according to the *F* and *K* parameters, while it is AOMP5 according to the *D* and *R* parameters.

When the findings obtained with this study are evaluated as a whole, it is understood once again that the effects of different parameters on the cross-section calculations cannot be ignored. In this context, it is a foregone conclusion that the use of advanced theoretical models in many evaluations, such as production cross–section calculations of radioisotopes, which are used in many aspects of our lives, particularly in industry and health, and provide numerous benefits, will provide significant contributions to researchers in cases where experimental studies are not doable. This and related studies are supposed to be carried out in order to improve/develop the model and parameters, to utilize them independently/together, to be chosen in line with the examined reaction, and to add to the literature by attempting numerous reactions.

Conflicts of interest

There are no conflicts of interest in this work.

References

[1] World Nuclear Association. Radioisotopes in Industry. Available at: https://www.world-nuclear.org/information-library/non-power-nuclear-applications/radioisotopes-research/radioisotopes-in-industry.aspx. Retrieved March 26, 2022.

[2] Das T., Pillai M.R.A., Options to Meet the Future Global Demand of Radionuclides for Radionuclide Therapy, *Nucl. Med. Biol.*, 40 (1) (2013) 23-32.

[3] Akkoyun S., Kaya H., Estimations of Cross-Sections for Photonuclear Reaction on Calcium Isotopes by Artificial Neural Network, *Sakarya University Journal of Science*, 24 (5) (2020) 1115-1120.

[4] Özdoğan H., Şekerci M., Kaplan A., An Investigation on the Effects of Some Theoretical Models in the Cross-Section Calculations of $^{50,52,53,54}Cr(\alpha,x)$ Reactions, *Phys. At. Nucl.*, 83 (6) (2020) 820-827.

[5] Şekerci M., Özdoğan H., Kaplan A., An Investigation of Effects of Level Density Models and Gamma Ray Strength Functions on Cross-Section Calculations for the Production of ^{90}Y, ^{153}Sm, ^{169}Er, ^{177}Lu and ^{186}Re Therapeutic Radioisotopes via (n,g) Reactions, *Radiochim. Acta*, 108 (1) (2020) 11-17.

[6] Şekerci M., Theoretical Cross-Section Calculations for the (α,n) and (α,2n) Reactions on ^{46}Ti, ^{50}Cr, ^{54}Fe, and ^{93}Nb Isotopes, *Mosc. Univ. Phys. Bull.*, 75 (2) (2020) 123-132.

[7] Akkoyun S., Bayram T., Production Cross-Section of ^{51}Cr Radioisotope Using Artificial Neural Networks, *Turkish Journal of Science and Health*, 2 (1) (2021) 133-138.

[8] Özdoğan H., Üncü Y.A., Karaman O., Şekerci M., Kaplan A., Estimations of Giant Dipole Resonance Parameters Using Artificial Neural Network, *Appl. Radiat. Isot.*, 169, (2021) 109581.

[9] Yiğit M., Study of Cross Sections for (n,p) Reactions on Hf, Ta and W Isotopes, *Appl. Radiat. Isot.*, 174, (2021) 109779.

[10] Stöcklin G., Qaim S.M., Rösch F., The Impact of Radioactivity on Medicine Metallic, *Radiochim. Acta*, 70/71 (1995) 249-272.

[11] Kaplan A, Sarpün İ.H., Aydın A., Tel E., Çapalı V., Özdoğan H., (γ,2n) Reaction Cross-Section Calculations of Several Even-Even Lanthanide Nuclei Using Different Level Density Models, *Phys. At. Nucl.*, 78 (2015) 53-64.

[12] Özdoğan H., Şekerci M., Kaplan A., Investigation of Gamma Strength Functions and Level Density Models Effects on Photon Induced Reaction Cross–Section Calculations for the Fusion Structural Materials $^{46,50}Ti$, ^{51}V, ^{58}Ni and ^{63}Cu". *Appl. Radiat. Isot.*, 143 (2019) 6-10.

[13] Şekerci M., An Investigation of the Effects of Level Density Models and Alpha Optical Model Potentials on the Cross-Section Calculations for the Production of the Radionuclides ^{62}Cu, ^{67}Ga, ^{86}Y and ^{89}Zr via Some Alpha Induced Reactions, *Radiochim. Acta*, 108 (6) (2019) 459-467.

[14] Şekerci M., Özdoğan H., Kaplan A., Investigation on the Different Production Routes of ^{67}Ga Radioisotope by Using Different Level Density Models, *Mosc. Univ. Phys. Bull.*, 74 (2019) 277-281.

[15] Özdoğan H., Üncü Y.A., Şekerci M., Kaplan A., Estimations of Level Density Parameters by Using Artificial Neural Network for Phenomenological Level Density Models, *Appl. Radiat. Isot.*, 169 (2021) 109583.

[16] Gülümser T., Kaplan A., A Theoretical Study on the Production Cross–Section Calculations for ^{24}Na Medical Isotope, *Erzincan Üniversitesi Fen Bilimleri Enstitüsü Dergisi*, 14 (2) (2021) 802-813.

[17] Sarpün İ.H., Özdoğan H., Taşdöven K., Yalim H.A., Kaplan A., Theoretical Photoneutron Cross-Section Calculations on Osmium Isotopes by Talys And Empire Codes, *Mod. Phys. Lett. A.*, 34 (26) (2019) 1950210.

[18] Şekerci M., Özdoğan H., Kaplan A., Level Density Model Effects on the Production Cross-Section Calculations of Some Medical Isotopes via (α,xn) Reactions where x=1–3, *Mod. Phys. Lett. A.*, 35 (24) (2020) 2050202.

[19] Özdoğan H., Şekerci M., Kaplan A., Photo-Neutron Cross-Section Calculations of ^{54,56}Fe, ^{90,91,92,94}Zr, ^{93}Nb and ^{107}Ag Isotopes with Newly Obtained Giant Dipole Resonance Parameters, *Appl. Radiat. Isot.*, 165 (2020) 109356.

[20] Özdoğan H., Estimation of (n,p) Reaction Cross Sections at 14.5±0.5 MeV Neutron Energy by Using Artificial Neural Network, *Appl. Radiat. Isot.*, 170 (2021) 109584.

[21] Weeks M.E., The discovery of the elements. XVII. The halogen family, *J. Chem. Educ.*, 9 (11) (1932) 1915.

[22] Greenwood N.N., Earnshaw A., Chemistry of the Elements. 2nd ed. United Kingdom: Oxford, (1997) 1-1364.

[23] Lide, D.R. (ed)., CRC Handbook of Chemistry and Physics. 85th ed. Florida, (2004) 1-2712.

[24] Rowland D.J., McCarthy T.J., Welch M.J., Radiobromine for Imaging and Therapy. In: Welch M.J., Redvanly C.S., (Eds). Handbook of Radiopharmaceuticals: Radiochemistry and Applications. John Wiley & Sons (2002) 441-465.

[25] Wilbur D.S., Adam M.J., Radiobromine and Radioiodine for Medical Applications, *Radiochim. Acta*, 107 (9-11) (2019) 1033–1063.

[26] Koning A., Hilaire S., Goriely S., TALYS–1.95 A Nuclear Reaction Program, User Manual. 1st ed. NRG, The Netherlands (2019).

[27] Daehnick W.W., Childs J.D., Vrcelj Z., Global Optical Model Potential for Elastic Deuteron Scattering from 12 to 90 MeV, *Phys. Rev. C.*, 21 (1980) 2253–2274.

[28] Bojowald J., Machner H., Nann H., Oelert W., Rogge M., Turek P., Elastic Deuteron Scattering and Optical Model Parameters at Energies up to 100 MeV, *Phys. Rev. C.*, 38 (1988) 1153–1163.

[29] Han Y., Shi Y., Shen Q., Deuteron Global Optical Model Potential for Energies up to 200 Mev, *Phys. Rev. C.*, 74 (2006) 044615.

[30] An H., Cai C., Global Deuteron Optical Model Potential for the Energy Range up to 183 MeV, *Phys. Rev. C.*, 73 (2006) 054605.

[31] McFadden L., Satchler G.R., Optical-Model Analysis of the Scattering of 24.7 MeV Alpha Particles, *Nucl. Phys.*, 84 (1966) 177–200.

[32] Demetriou P., Grama C., Goriely S., Improved Global α-optical Model Potentials at Low Energies, *Nucl. Phys. A.*, 707 (2002) 253–276.

[33] Avrigeanu V., Avrigeanu M., Mănăilescu C., Further Explorations of the α-particle Optical Model Potential at Low Energies for the Mass Range A≈45–209, *Phys. Rev. C.*, 90 (2014) 044612.

[34] Nolte M., Machner H., Bojowald J., Global Optical Potential for α particles with Energies Above 80 MeV, *Phys. Rev. C.*, 36 (1987) 1312.

[35] Avrigeanu V., Hodgson P.E., Avrigeanu M., Global Optical Potentials for Emitted Alpha Particles, *Phys. Rev. C.*, 49 (1994) 2136.

[36] Alabyad M., Mohamed G.Y., Hassan H.E., Takács S., Ditrói F., Experimental Measurements and Theoretical Calculations for Proton, Deuteron and α-Particle Induced Nuclear Reactions on Calcium: Special Relevance to the Production of ^{43,44}Sc, *J. Radioanal. Nucl. Chem.*, 316 (1) (2018) 119–128.

[37] Tárkányi F., Takács S., Ditrói F., Szűcs Z., Brezovcsik K., Hermanne A., Ignatyuk A.V., Investigation of Cross Sections of Deuteron Induced Nuclear Reactions on Selenium up to 50 MeV, *Eur. Phys. J.* A, 57 (4) (2021) 117.

[38] Otuka N., Dupont E., Semkova V., Pritychenko B., Blokhin A.I., Aikawa M., Babykina S., Bossant M., Chen G., Dunaeva S., Forrest R.A., Fukahori T., Furutachi N., Ganesan S., Ge Z., Gritzay O.O., Herman M., Hlavač S., Katō K., Lalremruata B., Lee Y.O., Makinaga A., Matsumoto K., Mikhaylyukova M., Pikulina G., Pronyaev V.G., Saxena A., Schwerer O., Simakov S.P., Soppera N., Suzuki R., Takács S., Tao X., Taova S., Tárkányi F., Varlamov V.V., Wang J., Yang S.C., Zerkin V., Zhuang Y., Towards a More Complete and Accurate Experimental Nuclear Reaction Data Library (EXFOR): International Collaboration Between Nuclear Reaction Data Centres (NRDC), *Nucl. Data Sheets*, 120 (2014) 272-276.

[39] Zerkin V.V., Pritychenko B., The experimental nuclear reaction data (EXFOR): Extended Computer Database and Web Retrieval System, *Nucl. Instrum. Methods. Phys. Res. A*, 888 (2018) 31–43.

[40] Levkovski V.N., Cross-Section of Medium Mass Nuclide Activation (A=40-100) by Medium Energy Protons and Alpha Particles (E=10-50 MeV), Inter-Vesi, Moscow, USSR (1991).